Time delay induced different synchronization patterns in repulsively coupled chaotic oscillators

Chenggui Yao, Ming Yi, and Jianwei Shuai

Citation: Chaos: An Interdisciplinary Journal of Nonlinear Science **23**, 033140 (2013); doi: 10.1063/1.4821942
View online: http://dx.doi.org/10.1063/1.4821942
View Table of Contents: http://scitation.aip.org/content/aip/journal/chaos/23/3?ver=pdfcov
Published by the AIP Publishing

Time delay induced different synchronization patterns in repulsively coupled chaotic oscillators

Chenggui Yao,[1,2,a)] Ming Yi,[3] and Jianwei Shuai[1]
[1]*Department of Physics and Institute of Theoretical Physics and Astrophysics, Xiamen University, Xiamen 361005, People's Republic of China*
[2]*Department of Mathematics, Shaoxing University, Shaoxing 312000, China*
[3]*Wuhan Institute of Physics and Mathematics, Chinese Academy of Sciences, Wuhan, China*

(Received 30 July 2013; accepted 8 September 2013; published online 20 September 2013)

Time delayed coupling plays a crucial role in determining the system's dynamics. We here report that the time delay induces transition from the asynchronous state to the complete synchronization (CS) state in the repulsively coupled chaotic oscillators. In particular, by changing the coupling strength or time delay, various types of synchronous patterns, including CS, antiphase CS, antiphase synchronization (ANS), and phase synchronization, can be generated. In the transition regions between different synchronous patterns, bistable synchronous oscillators can be observed. Furthermore, we show that the time-delay-induced phase flip bifurcation is of key importance for the emergence of CS. All these findings may light on our understanding of neuronal synchronization and information processing in the brain. © *2013 AIP Publishing LLC*. [http://dx.doi.org/10.1063/1.4821942]

Synchronization, an important topic in nonlinear science, has attracted attention of researchers in different research fields due to its potential application to physics, chemistry, biology, and secure communications. We here report that time delay can induce different synchronization patterns in repulsively coupled chaotic oscillators. In particular, the complete synchronization (CS) state can be observed in the repulsively coupled chaotic oscillators. We hope our result can provide insights into the dynamics of complex system.

I. INTRODUCTION

Recent years, the synchronization has attracted much attention in the field of nonlinear dynamics due to its key role in physics, biology, and sociology.[1] A variety of interesting problems on synchronization have been discussed, such as the analysis method for synchronization,[2,3] the applications of synchronization,[4,5] the stability conditions for synchronization,[6,7] and so on. In studies of synchronization of coupled nonlinear oscillators, different conditions have been considered, such as the periodic or chaotic unit, instantaneous or time-delayed coupling, and local or global coupling. A rich variety of synchronous phenomena have been found, including CS,[8–10] phase synchronization (PS),[11,12] generalized synchronization,[13] and lag synchronization.[14]

Most of these researches are focused on attractive coupling that the sign of coupling strength is positive since the entrainment between oscillators is one of the main concerns. However, it is known that the synchronization in neuronal oscillators can be improved by combination of excitatory, inhibitory synapse interactions and even repulsive coupling.[15–17] The oscillators with repulsive coupling of which the sign is negative usually repel each other resulting in out-phase behavior. This phenomenon has been verified experimentally in the electrically coupled biological neurons, and anti-phase synchronization was observed for the strong repulsive coupling.[18]

The unusual effect of repulsive coupling has been studied and many innovative phenomena have been found. For example, Yanagita *et al.* showed that a pair of excitable FitzHugh-Nagumo neurons can exhibit various firing patterns including multistability and chaotic firing when elements interact repulsively.[19] Toledano *et al.* reported that two-dimensional colloidal aggregation can be mediated by repulsive interactions.[20] Ito *et al.* studied intermittent switching behaviors in a system with three identical oscillators coupled diffusively and repulsively.[21] Martins *et al.* showed that the response of the systems to an external signal is optimal at a particular proportion of repulsive links.[22] The phase oscillators with both attractive and repulsive couplings have been investigated, and various synchronous patterns were found.[23,24] Interestingly, the synchronization can be enhanced by repulsive coupling.[17,25]

Time delay, arising from finite propagation speeds of signal transmission over a distance, has also been widely studied, and various phenomena have been uncovered in time-delayed coupling oscillators. Time delay can induce oscillation death and mutistable in limit cycle oscillators.[26–31] Kori *et al.* showed that the slow switching can be observed in globally delay-coupled phase oscillators.[32] Furthermore, time delay can also be as a method of controlling cluster and synchronization in the excitable Boolean networks and the large laser networks.[33,34] The appropriate time delays can induce the stable CS in a network of neuronal oscillators with attractive coupling.[35]

Recently, it has been shown that the synchronization degree can be improved periodically with increasing delay length for repulsive coupling in a neuronal network with periodically spiking neurons.[36] So far, to the best of our

a)Author to whom correspondence should be addressed. Email address: yaochenggui2006@126.com

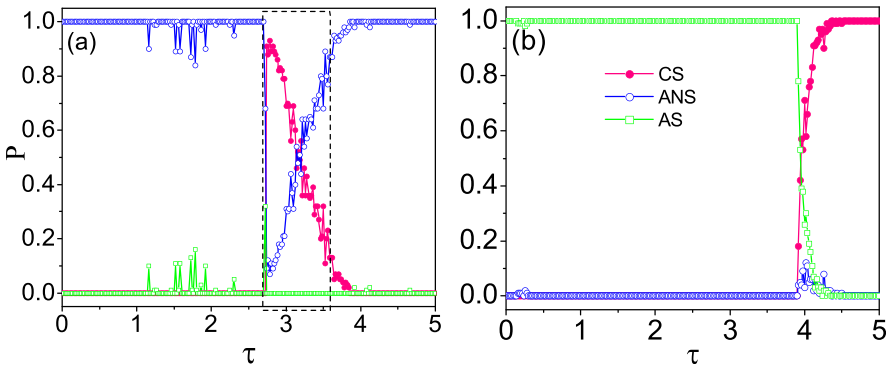

FIG. 1. (a) and (b) The probability P of anti-phase synchronization, complete synchronization, and asynchronization versus τ for $\epsilon = -2.5$ and $\epsilon = -0.5$, respectively. P is determined by averaging over 100 different sets of initial conditions.

knowledge, in all existing works on the repulsive coupling systems, the effects of interplays between repulsive coupling and time delay on the synchronization of chaotic oscillators were less considered.

In this paper, we study two pairs of repulsively coupled chaotic oscillators with time delay in the coupling interaction. We show that different synchronous patterns can occur with the different values of coupling strength and time delay. For the chaotic oscillators, the repulsive coupling can typically induce the antiphase synchronization (ANS) state. Surprisingly, we find that the time delay can drive the chaotic oscillators, which repel each other by repulsive interaction, to the stable CS state or PS state. We also find that the CS and ANS states occur alternatively with increasing delay length at suitable repulsive coupling strength. Furthermore, the phase-flip transition between in-phase and anti-phase which has been discussed in attractive coupling system[37–39] is also observed in our system with repulsive coupling. The paper will be arranged as follows: in Secs. II and III, two different types of classical oscillator models (Hindmarsh-Rose neuronal model and Lorenz oscillator) are studied and checked. Finally, we give a summary in Sec. IV.

II. THE HINDMARSH-ROSE NEURONAL MODEL

In the following, we first study a pair of repulsively coupled Hindmarsh-Rose neurons with time delay, which are given by the following equations:[41]

$$\dot{x}_i = y_i - ax_i^3 + bx_i^2 - z_i + I_{ext} + \epsilon(x_j(t-\tau) - x_i), \quad (1)$$

$$\dot{y}_i = c - dx_i^2 - y_i, \quad (2)$$

$$\dot{z}_i = r[s(x_i - x_0) - z_i], \quad (3)$$

where the indices $i = 1, 2$ and $j = 2, 1$, respectively. x is the membrane potential, y is the recovery variable, and z is the adaptation variable. r is the ratio of fast/slow time scales. I_{ext} is the external current input. The parameters setting $a = 1.0, b = 3.0, c = 1.0, d = 5.0, s = 4.0, r = 0.006, x_0 = -1.6$, and $I_{ext} = 3.3$ are chosen and fixed at which the uncoupled unit exhibits chaotic burst-spike behavior. ϵ and τ stand for coupling strength and time delay, respectively. Here, we consider repulsive coupling. Thus, the sign of coupling strength is negative, which implies that the smaller the coupling strength, the stronger the repelling interaction.

The initial conditions for x_i, y_i, z_i are chosen randomly from the interval [0, 1]. In order to discuss the situation of phase synchronization of the coupled elements, the phase of each oscillator is defined as

$$\phi(t) = 2k\pi + 2\pi\frac{t - t_{k-1}}{t_k - t_{k-1}} \quad (t_{k-1} < t < t_k), \quad (4)$$

where t_k is the time at which the kth bursting or spiking cycle begins. Our simulation results show that the systems behave three primary features: CS, anti-phase synchronization (ANS) which the phase difference of two oscillators is close to π and asynchronization (AS).

To clarify the effect of time delay on the repulsively coupled Hindmarsh-Rose neurons, we discuss the probabilities P of CS, ANS, and AS of the system at a given set of parameters with 100 random initial conditions, which are chosen randomly from the interval [0, 1]. Figs. 1(a) and 1(b) show how the three probabilities P change with time delay τ for $\epsilon = -2.5$ and $\epsilon = -0.5$, respectively. A surprising result given in the figure is that the sufficiently large time delay can induce CS between two oscillators. For the strong coupling, we can see that the two oscillators are mainly in ANS states when τ is small, but show CS behavior when τ is moderate [Fig. 1(a)]. For the weak coupling, however, time delay can induce system jump from AS to CS [Fig. 1(b)].

To get a global view, the phase diagram on the (ϵ, τ) plane is shown in Fig. 2. The ANS, AS, and CS region are

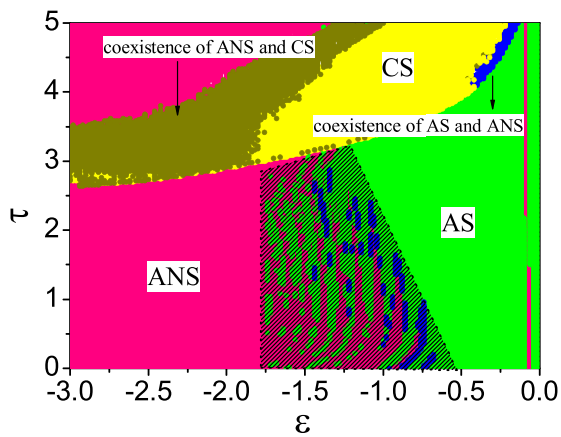

FIG. 2. Phase diagram on the (ϵ, τ) plane for different synchronous regions of the repulsively coupled Hindmarsh-Rose neuronal model (Eq. (1)). The letters CS, ANS, and AS stand for the complete synchronization, anti-phase synchronization, asynchronization, respectively. The coexistence regions of ANS and CS (AS) are indicated by the different colors.

determined by $P_{ANS} > 0.8$, $P_{AS} > 0.8$, and $P_{CS} > 0.8$, respectively; otherwise, the coexistence regions are defined. In Fig. 2, the green region corresponds to AS and here the two oscillators exhibit phase-drift behavior; the pink region corresponds to ANS. Interestingly, there exists a large region for CS which is represented by the yellow region. Some special regions, i.e., bistability regions of CS and ANS, are marked out. In the regime indicated by dense, the system exhibits more complex behavior.

To show the detailed dynamics, Figs. 3(a)–3(d) plot the time series of $x(t)$ for the system with randomly chosen model parameters in each region. Fig. 3(a) gives the anti-phase synchronous bursting, and Fig. 3(b) presents the complete synchronous spike. Fig. 3(c) shows out-phase chaotic solutions between two oscillators, while Fig. 3(d) is devoted to examples of coexistence of ANS and CS with different initial conditions in which the inset shows the CS state.

In order to discuss the dynamical behaviors in detail, the bifurcation of Δt_i which is defined as the inter-spike interval for different time delay is given in Fig. 4. At the small time delay, we can find clearly that the system transfers from the chaotic state to the periodic bursting with the increase of the coupling strength [Fig. 4(a)], and the period $n+1 \rightarrow$ period n bifurcation occurs in the periodic region [the zoomed-in part of Fig. 4(a)]. For the large time delay, however, the periodic spiking occurs at a larger range [Fig. 4(b)]. The dynamical phase diagram is plotted in Fig. 5 on the (ϵ, τ) plane. Comparing Fig. 5 with Fig. 2, we can get three interesting features: (i) the two oscillators at ANS fire with periodic bursting or spiking, (ii) the two oscillators which behave chaotic behavior are in AS state, and (iii) CS is usually achieved by periodic spiking. Furthermore, period $n+1 \rightarrow$ period n bifurcation is presented clearly in Fig. 5.

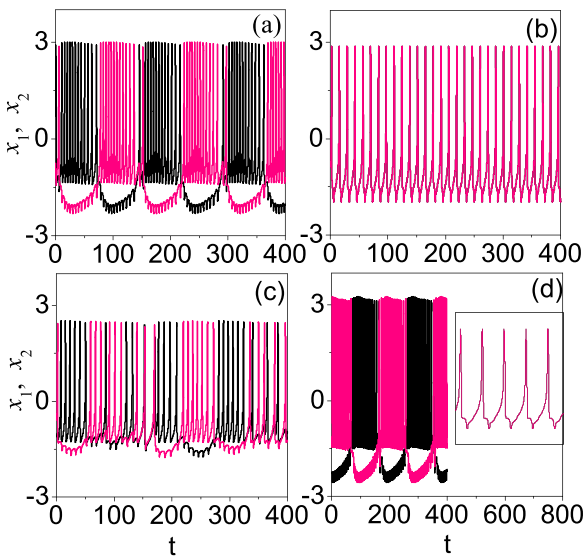

FIG. 3. (a)–(d) The time series of $x_1(t)$ (black line) and $x_2(t)$ (pink line) (a) of ANS with $(\epsilon, \tau) = (-1.5, 0.3)$, (b) of CS with $(\epsilon, \tau) = (-1.5, 3.3)$, (c) of AS with $(\epsilon, \tau) = (-0.74, 1.5)$ and (d) of coexistence of ANS AND CS with $(\epsilon, \tau) = (-2.0, 3.6)$.

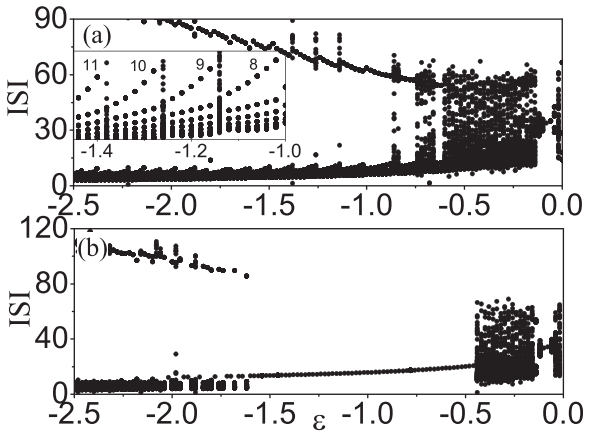

FIG. 4. (a) and (b) The bifurcation of Δt_i (the interval time of successive spikes) of $x_1(t)$ for $\tau = 0.5$ and $\tau = 4.0$, respectively. The inset of (a) shows the zoomed-in part of (a), indicating the $n+1 \rightarrow n$ bifurcation.

The underlying mechanism for the phase transition from ANS(AS) to CS can be understood well with Figs. 6(a)–6(d), which show the phase difference between two oscillators and the frequencies of two oscillators as a function τ for $\epsilon = -1.8$ and $\epsilon = -2.0$, respectively. Figs. 6(a) and 6(c) indicate that the phase difference abruptly changes from π to 0, indicating that the flip bifurcation occurs. This phenomenon has been observed widely in many systems with attractively coupled oscillators.[37–39] However, the two oscillators jump to the coexistence region of out-phase and in-phase for the large coupling strength (Fig. 6(c)). The left and right insets in Fig. 6(a) are representative trajectories at $\tau = 2.9$, before the bifurcation, and at $\tau = 3.1$, after the bifurcation, respectively. The oscillation frequency Ω (measured from the peak-to-peak separation) is also a key characteristic of the phase-flip bifurcation. Figs. 6(b) and 6(d) show the simultaneous jump of frequency.

III. THE LORENZ OSCILLATOR

In order to gain more insight into the role of time delay on synchronization of the repulsively coupled chaotic

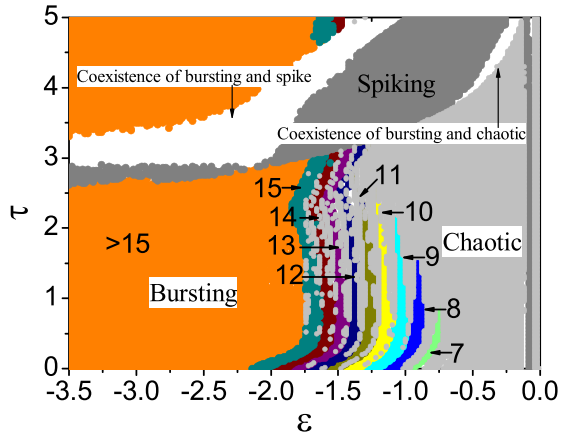

FIG. 5. Schematic phase diagram for Eq. (1) in the (ϵ, τ) plane for different dynamic parameter region. The chaotic state is determined by randomicity of Δt_i.

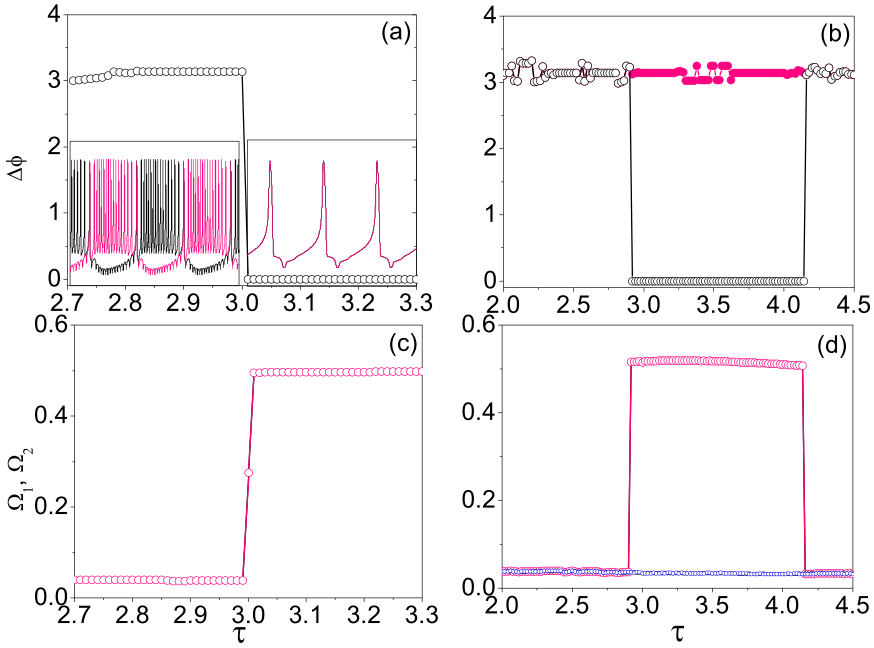

FIG. 6. The phase difference between the oscillators ((a) and (b)) and the frequency of the synchronized oscillators ((c) and (d)) as function of τ for $\epsilon = -1.8$ and $\epsilon = -2.0$, respectively. The trajectories before and after the transition are shown in the inset of (a).

oscillators, we investigate the repulsively coupled Lorenz chaotic oscillators with time delay, which can be expressed as

$$\dot{x}_i = a(y_i - x_i), \tag{5}$$

$$\dot{y}_i = bx_i - y_i - x_i z_i + \epsilon(y_j(t-\tau) - y_i), \tag{6}$$

$$\dot{z}_i = x_i y_i - c z_i, \tag{7}$$

where $i = 1, 2$ and $j = 2, 1$, respectively. $a = 10.0$, $b = 28.0$, and $c = 1.0$ at which the uncoupled oscillators have a stable chaotic attractor. The parameters ϵ and τ are free.

For this case, the phase of each oscillator is defined as

$$\phi_i(t) = \tan^{-1}[y_i'(t)/x_i'(t)], \tag{8}$$

where $x_i'(t) = \sqrt{x_i^2(t) + y_i^2(t)} \quad -\sqrt{2c(b-1)}$, $y_i'(t) = z_i(t) - (b-1)$,[40] and the phase difference between the oscillators is $\Delta\phi = \langle \phi_1(t) - \phi_2(t) \rangle$, with $\langle\rangle$ denoting the average over time. The initial conditions for x_i, y_i, z_i are chosen randomly from the interval $[-1, 1]$. Our simulation results show that four different synchronization behaviors can be observed in this system, including AS, ANS ($\Delta\phi = \pi$), CS, and PS with $\Delta\phi \neq \pi$. It is notable that this ANS is with $x_1(t) + x_2(t) = 0$.

Figures 7(a) and 7(b) plot the probabilities of AS, ANS, CS, and PS versus τ for $\epsilon = -3.8$ and $\epsilon = -2.0$, respectively. Surprisingly, we find that the CS and ANS emerge alternately for the strong coupling when the time delay τ increases, and the PS only exists at a small interval [Fig. 7(a)]. For the weak coupling, the AS is observed for the arbitrary initial conditions [Fig. 7(b)].

Figure 8 shows the phase diagram on the plane (ϵ, τ) with four types of well divided regions. The ANS, AS, PS, and CS regions are determined by probabilities $P_{ANS} > 0.8$, $P_{AS} > 0.8$, $P_{PS} > 0.8$, and $P_{CS} > 0.8$, respectively. From this figure, we find that most of the parameter region is filled with AS state, which occurs at large coupling strength. Interestingly, the CS and ANS are observed alternatively with the increasing time delay at ϵ around -4. The boundary structures of ANS and CS are complex.

Now, we turn to the detailed dynamics. The time series of $x(t)$ for two oscillators are shown in Figs. 9(a)–9(d) for the parameters in four different regions. In Fig. 9(a), the two AS oscillators perform the chaotic behavior; while in Fig. 9(b), the two CS oscillators are in periodic state. Fig. 9(c) plots

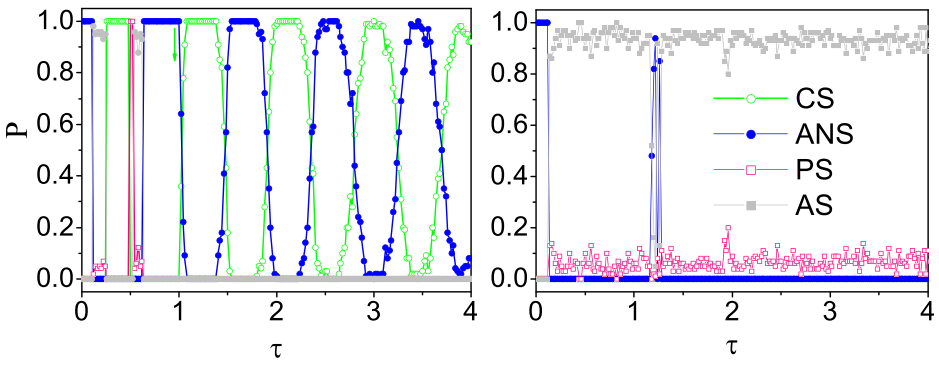

FIG. 7. (a) and (b) The probability P of anti-phase synchronization, complete synchronization, phase synchronization, and asynchronization versus τ for $\epsilon = -3.8$ and $\epsilon = -2.0$, respectively. P is determined by averaging over 100 different sets of initial conditions.

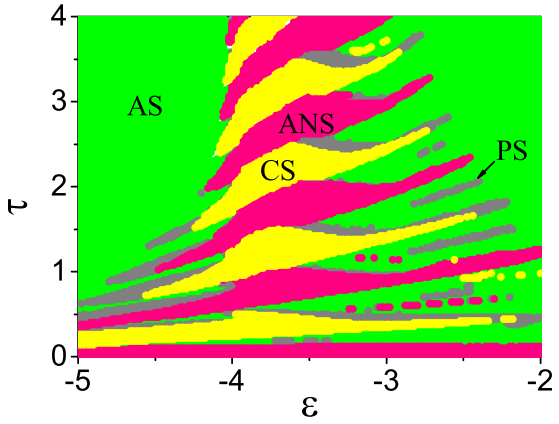

FIG. 8. Phase diagram on the (ϵ, τ) plane for different synchronous regions of the repulsively coupled Lorenz systems (Eq. (2)). The parameter space is separated into four regions, which correspond to phase synchronous (PS), asynchronous (AS), complete synchronous (CS), and anti-phase synchronous (ANS), respectively.

the two periodic oscillators, which are in ANS state. It is interesting that the time series of $x(t)$ for the two ANS oscillators are symmetrical about the $x=0$, which means $x_1(t) = -x_2(t)$. Fig. 9(d) shows the periodic oscillators, which are in PS state. Our simulation result indicates that the PS state can be found with either periodic or chaotic attractor at different parameter regions.

In the following, we suggest that the time-delay-induced phase-flip bifurcation may be responsible for the occurrence of CS. The phase difference between two oscillators as a function of delay is shown in Fig. 10(a) at $\epsilon = -3.5$. From this figure, one can find the successive phase transition behavior from in-phase to anti-phase with τ increasing over the each critical value τ_{ci}, where $i = 1, 3$ (or $i = 2, 4$) are the critical values of transition from ANS to CS (or from CS to ANS), and the frequencies Ω of the two oscillators jump abruptly as the oscillations switch from the in-phase to the anti-phase [Fig. 10(b)]. Those phase transitions are shown in Fig. 11(a) in which the bifurcations of the local maximal values for $x_1(t) - x_2(t)$ (blue circle points) and $x_1(t) + x_2(t)$ (pink solid points) are plotted. The two oscillators jump back and forth between the anti-phase state and the in-phase state with τ increasing. If we take a closer look at the region of ANS in Fig. 11(a), a specific antiphase synchronous state, antiphase CS, is also found. For antiphase CS, the two oscillators not only show a behavior of ANS but also have the same oscillating amplitude. As a result, a simple symmetric relationship $x_1(t) = x_2(t + T/2)$ is observed between the two oscillators with T the oscillating period. Furthermore, the

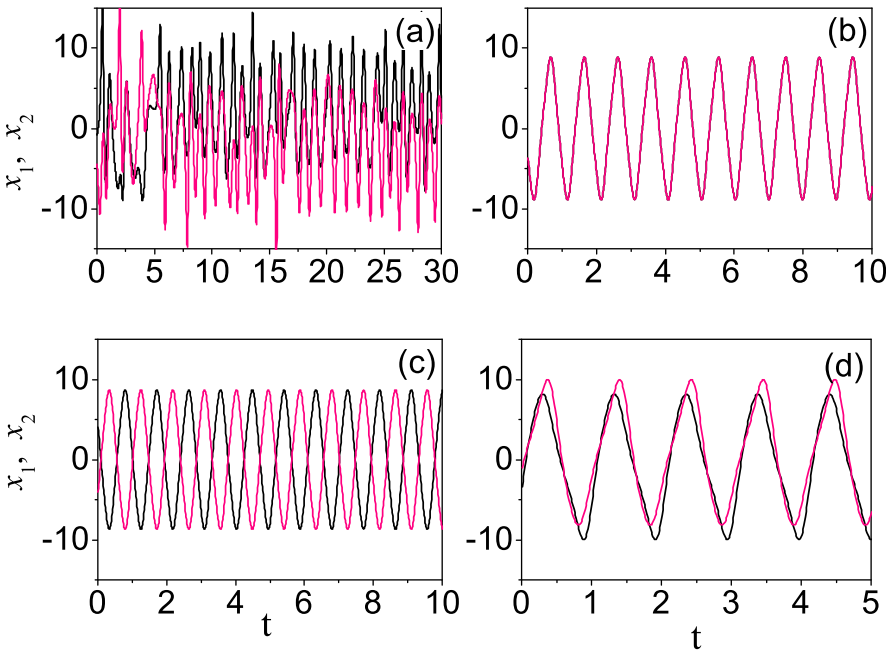

FIG. 9. (a)–(d) The time series of $x_1(t)$ (black line) and $x_2(t)$ (pink line) for $(\epsilon, \tau) = (-3.5, 0.2)$ (a), $(\epsilon, \tau) = (-3.5, 0.4)$ (b), $(\epsilon, \tau) = (-3.5, 0.8)$ (c), and $(\epsilon, \tau) = (-3.5, 1.5)$ (d), respectively.

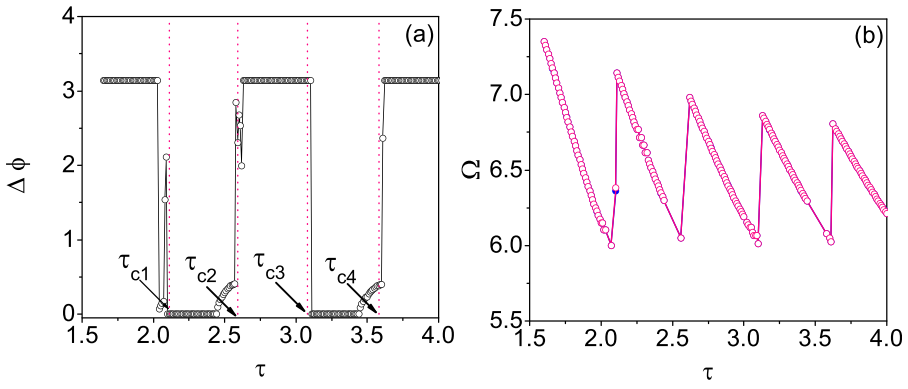

FIG. 10. The phase difference $\Delta\phi$ (a) and the frequency Ω (b) of the oscillators as a function of τ, some parameters for chaotic state are deleted. $\epsilon = -3.5$.

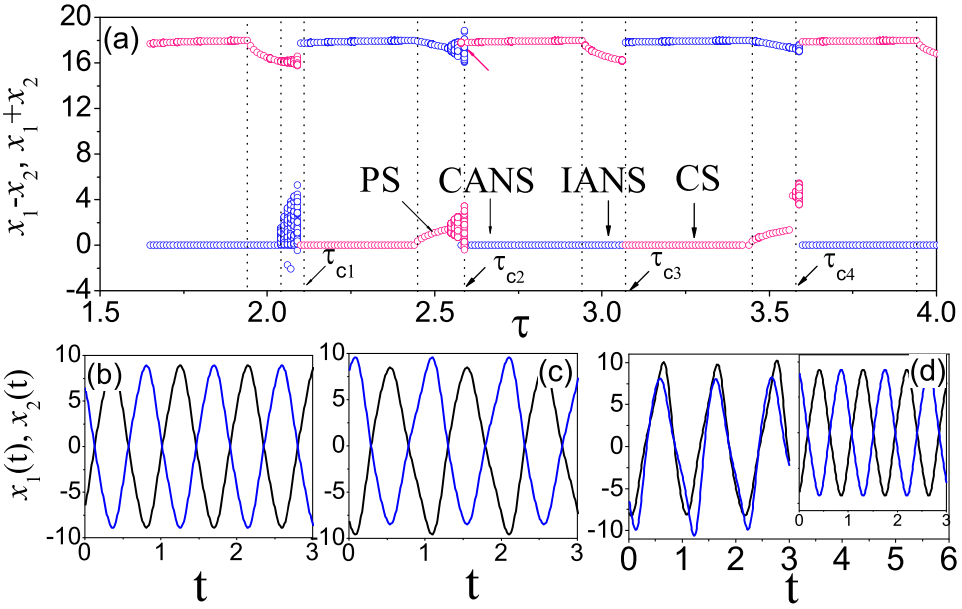

FIG. 11. (a) The bifurcation of $x_1(t) + x_2(t)$ (the blue points) and $x_1(t) - x_2(t)$ (the pink points) for the local maximal values, showing the phase transition from anti-phase to in-phase. The letters CANS and IANS stand for the complete ANS and incomplete ANS, respectively. $\epsilon = -3.5$. (b) and (c) The time series of $x_1(t)$ and $x_2(t)$ for $(\epsilon, \tau) = (-3.5, 1.7)$ and $(-3.5, 1.97)$, respectively, giving an antiphase CS and a general ANS, respectively. (d) The time series of $x_1(t)$ and $x_2(t)$ for $(\epsilon, \tau) = (-3.5, 2.59)$, indicating coexistence of ANS and PS. The inset of (d) shows the effect of the different initial conditions.

bistable states (coexistence of ANS and PS) marked by pink arrow can be observed around τ_{ci} [Fig. 11(d)].

IV. CONCLUSION

The effect of time delay on the synchronization of the repulsively coupled chaotic oscillators is investigated systematically in the paper. Our numerical results reveal that such a system can show rich dynamic phenomena. Various synchronization patterns, including complete synchronization, antiphase complete synchronization, antiphase synchronization, and phase synchronization, are observed with varying repulsively coupling strength and time delay. Among the transition region of different synchronization states, the bistable synchronous states can be found. For the repulsively coupled Hindmarsh-Rose neuronal model with time delay, the anti-phase bursting synchronization, complete synchronous spiking, asynchronous chaotic state are uncovered. For the repulsively coupled Lorenz systems, time delay induce systems transition from anti-phase with $x_1(t) = -x_2(t)$ to the in-phase with $x_1(t) = x_2(t)$. Furthermore, we have indicated that the underlying mechanism of complete synchronization is time-delay-induced phase flip bifurcation. In the physical or biological systems, time delayed signals are unavoidable due to the finite transmission speeds. We hope our results can extend to coupled dynamical systems with general nonlinearities and provide further insight into information processing in biological systems.

ACKNOWLEDGMENTS

This work was partially supported by the National Natural Science Foundation of China under Grants No. 11205103 (C. G. Yao), Nos. 10905089 and 11275259 (M. Yi); the China National Funds for Distinguished Young Scientists under Grant No. 11125419; and the Training Program of Fujian Excellent Talents in University (J. W. Shuai).

[1]A. Pikovsky, M. Rosenblum, and J. Kurths, *Synchronization: A Universal Concept in Nonlinear Dynamics* (Cambridge University Press, Cambridge, England, 2001).
[2]W. Zhang, Y. Tang, Q. Miao, and W. Du, IEEE Trans. Neural Netw. Learn. Syst. **24**, 1316 (2013).
[3]Y. Tang and W. K. Wong, IEEE Trans. Neural Netw. Learn. Syst. **24**, 435 (2013).
[4]Y. Tang, H. Gao, W. Zou, and J. Kurths, IEEE Trans. Cybern. **43**, 358 (2013).
[5]Y. Tang, Z. Wang, H. Gao, S. Swift, and J. Kurths, IEEE/ACM Trans. Comput. Biol. Bioinf. **9**, 1569 (2012).
[6]W. Zou and M. Zhan, Europhys. Lett. **81**, 10006 (2008).
[7]W. Zou and M. Zhan, Chaos **18**, 043115 (2008).
[8]M. Zhan, G. Hu, and J. Yang, Phys. Rev. E **62**, 2963 (2000).
[9]J. W. Shuai, K. W. Wong, and L. M. Cheng, Phys. Rev. E **56**, 2272 (1997).
[10]C. G. Yao, Q. Zhao, and J. Yu, Phys. Lett. A **377**, 370 (2013).
[11]M. G. Rosenblum, A. S. Pikovsky, and J. Kurths, Phys. Rev. Lett. **76**, 1804 (1996).
[12]J. W. Shuai and D. M. Durand, Phys. Lett. A **264**, 289 (1999).
[13]L. Kocarev and U. Parlitz, Phys. Rev. Lett. **76**, 1816 (1996).
[14]M. G. Rosenblum, A. S. Pikovsky, and J. Kurths, Phys. Rev. Lett. **78**, 4193 (1997).
[15]N. Kopell and B. Ermentrout, Proc. Natl. Acad. Sci. U.S.A. **101**, 15482 (2004).
[16]M. Bartos, I. Vida, and P. Jonas, Nat. Rev. Neurosci. **8**, 45 (2007).
[17]I. Leyva, I. SendinNadal, J. A. Almendral, and M. A. F. Sanjuan, Phys. Rev. E **74**, 056112 (2006).
[18]R. C. Elson, A. I. Selverston, R. Huerta, N. F. Rulkov, M. I. Rabinovich, and H. D. I. Abarbanel, Phys. Rev. Lett. **81**, 5692, (1998).
[19]T. Yanagita, T. Ichinomiya, and Y. Oyama, Phys. Rev. E **72**, 056218 (2005).
[20]J. C. F. Toledano, A. Moncho-Jorda, F. M. Lopez, A. E. Gonzalez, and R. H. alvarez, Phys. Rev. E **75**, 041408 (2007).
[21]K. Ito and Y. Nishiura, Phys. Rev. E **77**, 036224 (2008).
[22]T. Vaz Martins, V. N. Livina, A. P. Majtey, and R. Toral, Phys. Rev. E **81**, 041103 (2010).
[23]D. H. Zanette, Europhys. Lett. **72**, 190 (2005).
[24]H. Hong and S. H. Strogatz, Phys. Rev. Lett. **106**, 054102 (2011).
[25]T. Vaz Martins and R. Toral, Prog. Theor. Phys. **126**, 353 (2011).
[26]H. G. Schuster and P. Wagner, Prog. Theor. Phys. **81**, 939 (1989).
[27]W. Zou and M. Zhan, Phys. Rev. E **80**, 065204 (2009).
[28]D. V. R. Reddy, A. Sen, and G. L. Jhonston, Phys. Rev. Lett. **80**, 5109 (1998).
[29]W. Zou, X. Zheng, and M. Zhan, Chaos **21**, 023130 (2011).
[30]S. H. Strogatz, Nature (London) **394**, 316 (1998).
[31]W. Zou, D. V. Senthilkumar, M. Zhan, and J. Kurths, Phys. Rev. Lett. **111**, 014101 (2013).
[32]H. Kori and Y. Kuramoto, Phys. Rev. E **63**, 046214 (2001).
[33]M. Nixon, M. Fridman, E. Ronen, A. A. Friesem, N. Davidson, and I. Kanter, Phys. Rev. Lett. **108**, 214101 (2012).
[34]D. P. Rosin, D. Rontani, D. J. Gauthier, and E. Schöll, Phys. Rev. Lett. **110**, 104102 (2013).

[35]M. Dhamala, V. K. Jirsa, and M. Ding, Phys. Rev. Lett. **92**, 074104 (2004).
[36]Q. Y. Wang, G. R. Chen, and M. Perc, PLoS ONE **6**, 15851 (2011).
[37]A. Prasad, J. Kurths, S. K. Dana, and R. Ramaswamy, Phys. Rev. E **74**, 035204 (2006).
[38]J. M. Cruz, J. Escalona, P. Parmananda, R. Karnatak, A. Prasad, and R. Ramaswamy, Phys. Rev. E **81**, 046213 (2010).
[39]R. Karnatak, N. Punetha, A. Prasad, and R. Ramaswamy, Phys. Rev. E **82**, 046219 (2010).
[40]J. L. Hindmarsh and R. M. Rose, Proc. R. Soc. London, Ser. B **221**, 87 (1984).
[41]Z. G. Zheng, *Collective Behaviors and Spatiotemporal Dynamics in Coupled Nonlinear Systems* (Higher Education Press, Beijing, 2004).